

A Novel Vinculin Binding Site of the IpaA invasin of *Shigella*

HaJeung Park[¶], Cesar Valencia-Gallardo[§], Andrew Sharff[‡], Guy Tran Van Nhieu[§],
and Tina Izard^{¶1}

From the [¶]Cell Adhesion Laboratory, Department of Cancer Biology, The Scripps Research Institute, Jupiter, Florida 33458, USA; the [§]CIRB, Collège de France, Unité de Communications Intercellulaires et Infections Microbiennes, DR2 Inserm U971, 75005 Paris Cedex, France; and [‡]Global Phasing Ltd, Sheraton House, Castle Park, Cambridge CB3 0AX, England

¹To whom correspondence should be addressed

SUPPLEMENTARY METHODS

Cloning, expression, and purification of IpaA(45-633) – The cDNA encoding residues 45 to 633 of IpaA was amplified by PCR from a virulence plasmid derived from the *Shigella flexneri* ΔIpaBC strain. We removed the *N*-terminal chaperone-binding domain (residues 1-44) to improve the solubility of IpaA. The PCR product was cloned into the *NdeI/EcoRI* restriction sites of the pET30a vector (Novagen) to generate pET30a-IpaA45-633. A heptahistidine-tag was added to the *C*-terminus to facilitate purification. The plasmid was then transformed into *E. coli* BL21(DE3) strain (Novagen). BL21(DE3) cells harboring pET30a-IpaA(45-633) were grown in auto-induction media (24) overnight at 30 °C. The cells were harvested and sonicated in an ice bath. After centrifugation at 10,000 x *g* for 20 min, the pellet was solubilized by resuspension in 6 M urea followed by centrifugation at 20,000 x *g* for 20 min. The supernatant was loaded onto a His-Trap HP chelating affinity chromatography column (GE Healthcare) pre-equilibrated with 6 M urea and 5 mM imidazole (pH 8). The column was washed with 40 column volumes of the equilibration buffer. IpaA 45-633 was eluted with 10 mM Tris-HCl (pH 8), 50 mM imidazole, 300 mM NaCl, 1 mM DTT, and 30 mM L-Arg. IpaA 45-633 was concentrated to ~4 mg/ml.

Analytical size exclusion chromatography – To determine the total number of available VBSs in IpaA that can bind to vinculin, we determined the stoichiometry of the interaction, by incubating almost full-length IpaA (residues 45-633) with increasing amounts of Vh1 and then analyzing the complex using analytical size exclusion chromatography. Protein samples (200 μl) containing IpaA and Vh1 at molar ratios of 1:5, 1:4, 1:3, 1:2, and 1:1, as well as IpaA alone and Vh1 alone were prepared by dilution in running buffer (10 mM Tris-HCl [pH 7.5], 150 mM NaCl, 50 mM L-Arg, and 2 mM DTT). L-Arg was necessary to prevent aggregation. The prepared samples were incubated at room temperature for 20 min before they were loaded onto a Superdex 200 10 x 3000 (GE Healthcare) analytical sizing chromatography column at a flow rate of 0.5 ml/min using an Äkta FPLC system (GE Healthcare). Peak fractions were collected and analyzed by SDS-PAGE.

FIGURE LEGENDS

Supplementary Figure S1. Temperature factor plot of IpaA-VBS3. The temperature factor for each C α IpaA-VBS3 atom is plotted in red and blue, respectively, for the two IpaA-VBS3 molecules in the asymmetric unit.

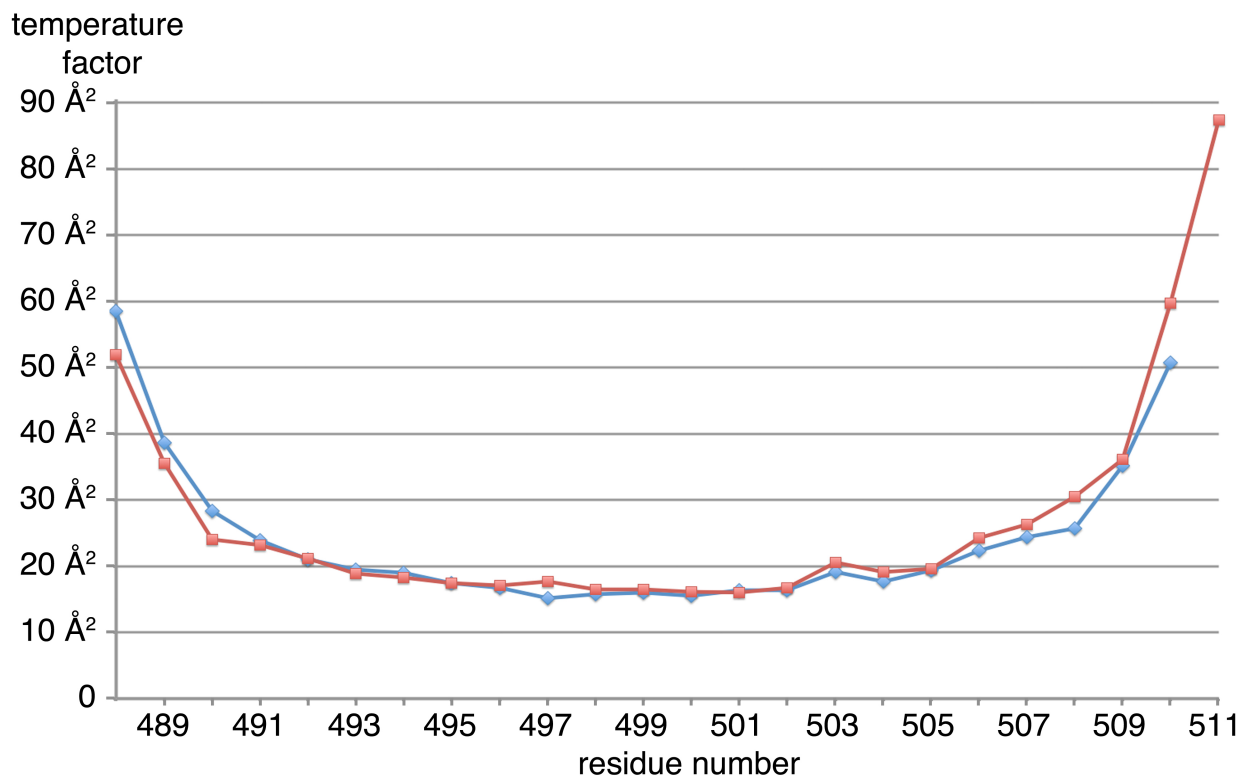
Supplementary Figure S2. Comparison of IpaA-VBS3 and IpaA-VBS1 interactions with Vh1. The Vh1:IpaA-VBS1 interactions are based on the 2.72 Å crystal structure (PDB entry 2gww), and this was compared to our 1.6 Å Vh1:IpaA-VBS3 structure presented here. IpaA-VBS3 (A) or IpaA-VBS1 (B) residues are labeled in blue while Vh1 interacting residues are labeled in black. Vh1 residues listed on the left of IpaA-VBS engage in polar inter-molecular interactions, while Vh1 residues listed on the right of IpaA-VBS residues engage in hydrophobic inter-molecular interactions. Structurally equivalent IpaA-VBS3 and IpaA-VBS1 residues are on the same line (*e.g.*, IpaA-VBS3 residue Ile-492 corresponds to IpaA-VBS1 residue Ile-612). The greater number of residues involved in the Vh1-IpaA-VBS3 interface is reflected in about 10% increase in buried surface area.

Supplementary Figure S3. Comparison of IpaA-VBS3 and IpaA-VBS2 interactions with Vh1. The Vh1:IpaA-VBS2 interactions are based on the 3.97 Å crystal structure (PDB entry 2hsq), and this was compared to our 1.6 Å Vh1:IpaA-VBS3 structure presented here. IpaA-VBS3 (A) or IpaA-VBS2 (B) residues are labeled in blue while Vh1 interacting residues are labeled in black. Vh1 residues listed on the left of IpaA-VBS engage in polar inter-molecular interactions, while Vh1 residues listed on the right of IpaA-VBS residues engage in hydrophobic inter-molecular interactions. Structurally equivalent IpaA-VBS3 and IpaA-VBS2 residues are on the same line (*e.g.* IpaA-VBS3 residue Ile-492 corresponds to IpaA-VBS2 residue Ile-566).

Supplementary Figure S4. Stoichiometry of the Vh1: IpaA complex as determined by size exclusion chromatography. Constant IpaA (residues 45-633) amounts were mixed with increasing molar ratios of Vh1. IpaA to Vh1 molar ratios were (A) 1:5, (B) 1:4, (C) 1:3, (D) 1:2, and (E) 1:1. IpaA alone (F) and Vh1 alone (G, shown twice for clarity) are also shown. Samples were applied to a Superdex 200 10 x 300 sizing chromatography column. The position of the absorption peak corresponding to the IpaA:Vh1 complex advanced (IpaA:Vh1 molar ratio of 1:0, the green dotted line indicates its peak position; 1:1, red; 1:2, blue; 1:3, grey) until the IpaA:Vh1 molar ratio reaches 1:3 and IpaA is saturated. Thus, IpaA can simultaneously bind up to three molecules of Vh1. The absorption peak of free Vh1 (orange dotted line) appears at a molar IpaA:Vh1 ratio of 1:4 (B) and 1:5 (A).

Supplementary Figure S5. SDS-PAGE analysis of peak fractions from the size exclusion chromatography experiment. The identity of the peaks from the size exclusion chromatography experiment (Fig. S4) was confirmed by 8% - 25% gradient SDS-PAGE. *Lanes* 1 and 2, samples were taken at 10 ml elution corresponding to the saturated Vh1:IpaA complex ($M_r = 154$ kDa), *lanes* 3 and 4 at 10.9 ml corresponding to IpaA alone (residues 45-633, $M_r = 67$ kDa), and *lanes* 5 and 6 at 15.2 ml corresponding to Vh1 alone (residues 1-258, $M_r = 29$ kDa).

Supplementary Figure S1



Supplementary Figure S2

A

polar Vh1	IpaA-VBS3	hydrophobic interactions Vh1
E60	R489	E60
M53	E490	
	T491	V57
	I492	L54, V57, G58, F126
	F493	T8, I12, L123
	E494	
	A495	L54, V57
	S496	I12, T119
S11, E14	K497	I12
	K498	A50
	V499	A50, V51, L54, I115
	T500	V16
	N501	
	S502	V47
	L503	V16, I20, S112, I115
Q19	S504	V16
	N505	
	L506	L40, P43, V44, L88
	I507	V16, I20, L23
Q19	S508	
	L509	L40, P43
	I510	L108

B

polar Vh1	IpaA-VBS1	hydrophobic interactions Vh1
	I612	V57, F126
	Y613	T8, L123, F126
	K614	
	A615	L54
	A616	I12, L123
	K617	
	D618	A50
	V619	A50, V51, I115
I12	T620	L13, V16
	T621	
	S622	A46, V47
	L623	V16
Q19	S624	V16, Q19
	K625	
	V626	P43
	L627	I20

Supplementary Figure S3

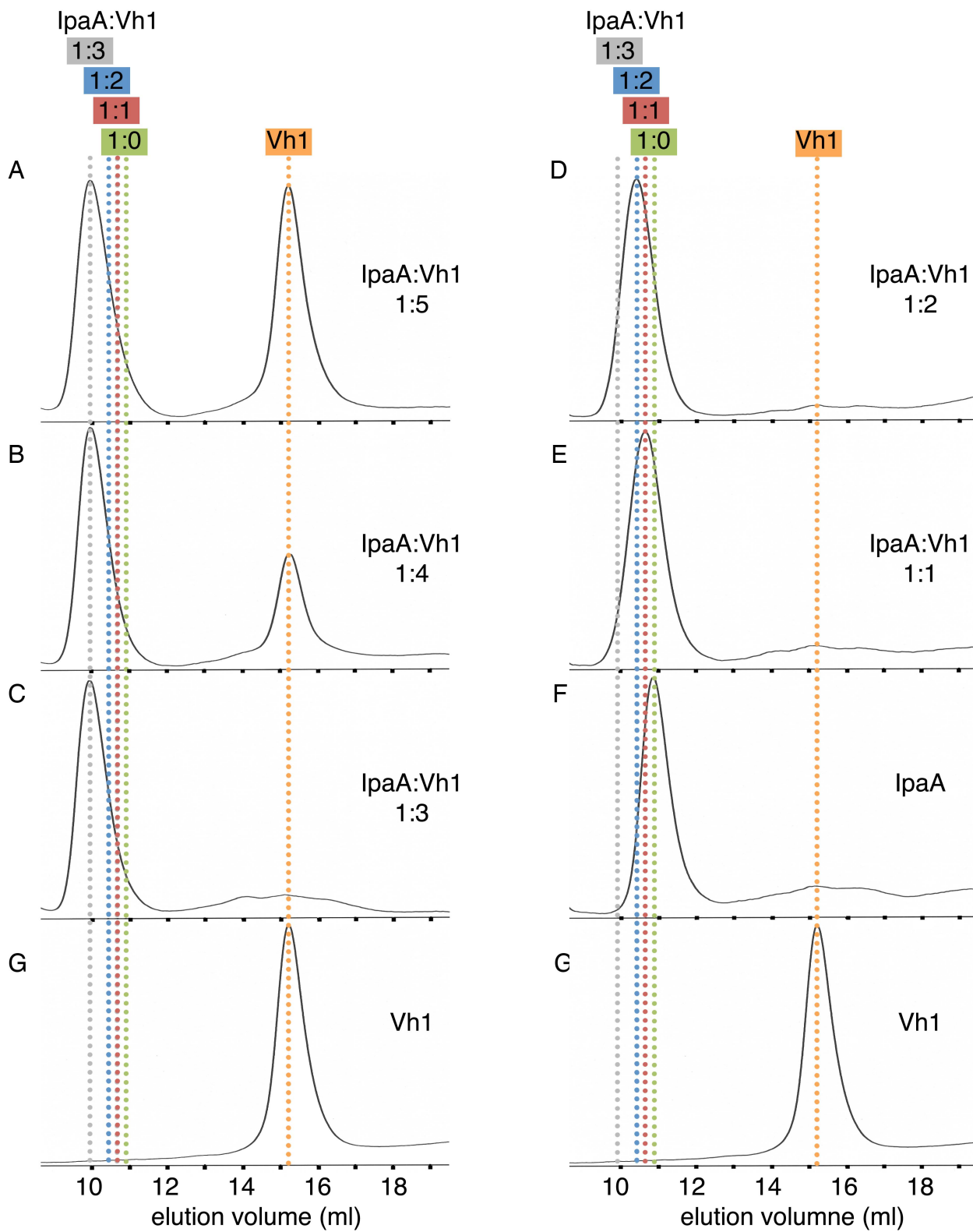
A

polar Vh1	IpaA-VBS3	hydrophobic interactions Vh1
E60	R489	E60
M53	E490	
	T491	V57
	I492	L54, V57, G58, F126
	F493	T8, I12, L123
	E494	
	A495	L54, V57
	S496	I12, T119
S11, E14	K497	I12
	K498	A50
	V499	A50, V51, L54, I115
	T500	V16
	N501	
	S502	V47
	L503	V16, I20, S112, I115
Q19	S504	V16
	N505	
	L506	L40, P43, V44, L88
	I507	V16, I20, L23
Q19	S508	
	L509	L40, P43
	I510	L108

B

polar Vh1	IpaA-VBS2	hydrophobic interactions Vh1
	A565	V57
	I566	L123, F126
D127	Y567	T8, I9, L123, F126
	E568	
	K569	L54, V57
	A570	L54, L123
	K571	I12
	E572	
	V573	A50, V51
I12	S574	
	S575	
	A576	
	L577	V16, V47, I88, S112
Q19	S578	
	K579	
	V580	P43, V44
	L581	V16, I20, S112
	S582	
	K583	L37, P38, L40
	I584	L23, I37, L40
	D585	L23

Supplementary Figure S4



Supplementary Figure S5

